A New Design Approach for a Compact Microstrip Diplexer with Good Passband Characteristics

Abbas Rezaei[1] and Salah I. Yahya[2,3]

[1]Department of Electrical Engineering, Kermanshah University of Technology, Kermanshah, Iran

[2]Department of Communication and Computer Engineering, Cihan University-Erbil, Erbil, Kurdistan region – F.R. Iraq

[3]Department of Software Engineering, Faculty of Engineering, Koya University, Koya KOY45, Kurdistan region – F.R. Iraq

***Abstract*—This paper presents an efficient theoretical design approach of a very compact microstrip diplexer for modern wireless communication system applications. The proposed basic resonator is made of coupled lines, simple transmission line and a shunt stub. The coupled lines and transmission line make a U-shape resonator while the shunt stub is loaded inside the U-shape cell to save the size significantly, where the overall size of the presented diplexer is only 0.008 λg^2. The configuration of this resonator is analyzed to increase intuitive understanding of the structure and easier optimization. The first and second resonance frequencies are f_{o1} = 895 MHz and f_{o2} = 2.2 GHz. Both channels have good properties so that the best simulated insertion loss at the first channel (0.075 dB) and the best simulated common port return losses at both channels (40.3 dB and 31.77 dB) are achieved. The presented diplexer can suppress the harmonics acceptably up to 3 GHz (3.3 f_{o1}). Another feature is having 31% fractional bandwidth at the first channel.**

***Index Terms*—Compact, Diplexer, Insertion loss, Microstrip, Resonator, Return loss**.

I. Introduction

Recently, microstrip devices such as diplexers have been used widely in modern wireless communication systems. Two-channel bandpass-bandpass diplexers can transmit signals through two passbands and eliminate undesired harmonics. Each channel is used for receiving or sending signals from an antenna (Majdi and Mezaal, 2022). Several types of microstrip diplexer are introduced in (Hussein, Mezaal and Alameri, 2021; Chen, et al., 2021; Yahya, Rezaei and Nouri, 2020; Lu, et al., 2020; Su, et al., 2020; Tahmasbi, Razaghian and Roshani, 2021; Rezaei, et al., 2019; Shirkhar and Roshani, 2021; Zhanga, Zhu and Li, 2018; Rezaei, Yahya, Noori and Jamaluddin, 2019; Dembele, et al., 2019; Yousif and Ezzulddin, 2020; Fernandez-Prieto, et al., 2018; Guan, et al., 2019; Guan, et al., 2014; Noori and Rezaei, 2017). However, all of them occupy large area. Two bandpass filters (BPFs) consisting spiral cells and coupled lines are integrated for obtaining a microstrip diplexer in (Hussein, Mezaal and Alameri, 2021). It has some disadvantages such as undesired harmonics and high losses at both channels. Three coupled lines structures are employed in the layout configuration of presented microstrip diplexer in (Chen, et al., 2021). It could better suppress harmonics but the problem of high losses at both channels is remained. The proposed diplexer in (Yahya, Rezaei and Nouri, 2020) could improve the simulated insertion losses at both channels while it could suppress the harmonics very well. However, it has two high common port return losses at both channels. In (Lu, et al., 2020), a microstrip diplexer with multiple transmission zeroes (TZs) has been designed to operate at 0.755 GHz and 1.056 GHz which is suitable for the Global System for Mobile Communications (GSM). The introduced diplexer in (Su et al., 2020) has large losses at both channels, but in (Tahmasbi, Razaghian and Roshani, 2021) the simulated insertion losses at both channels are very low. However, the proposed structure in (Tahmasbi, Razaghian and Roshani, 2021) could not obtain low return losses at its upper and lower channels. In (Rezaei, et al., 2019), sharpness is not good while it could not attenuate the harmonics. In (Shirkhar and Roshani, 2021), coupled meandrous structure has been employed to improve simulated insertion losses. However, it has undesired harmonics. A balanced-to-balanced microstrip diplexer using a large dual-mode resonator with undesired harmonics and high losses has been presented in (Zhanga, Zhu and Li, 2018). Two similar BPFs with flat channels are integrated in (Dembele, et al., 2019) for obtaining a microstrip bandpass-bandpass diplexer. In (Yousif and Ezzulddin, 2020), the microstrip meandrous closed loops have been utilized to design of a diplexer with good measured return losses. The problem of high losses has been remained in the presented diplexers in

ARO-The Scientific Journal of Koya University
Vol. X, No. 2 (2022), Article ID: ARO.10999. 6 pages
DOI: 10.14500/aro.10999
Received: 03 June 2022; Accepted: 28 July 2022
Regular research paper: Published: 25 August 2022
Corresponding author's email: a.rezaee@kut.ac.ir

 http://dx.doi.org/10.14500/aro.10999

(Fernandez-Prieto, et al., 2018; Guan, et al., 2019; Guan, et al., 2014; Noori and Rezaei, 2017).

While efforts are being made to design a compact microstrip bandpass-bandpass diplexer with good performance, it is hard to compromise the compact size on account of the design features, e.g., low losses, higher harmonics suppression and higher fractional bandwidth. The approach presented here is an efficient one which first, presents and analyzes a resonator. Second, this resonator is used to design two BPFs. Third, the BPFs are optimized so as to be integrated to achieve an efficient diplexer design. Finally, the proposed diplexer design is compared with the previous reported designs in terms of losses, size and harmonics, to prove the efficiency and better performance of the presented compact design. It has the best passbands totally.

II. Resonator Structure

Coupled lines are important parts of bandpass resonators. Because they create many capacitors between the lines, where both lines show inductance features. However, if we use only coupled lines, the dimensions will be very large, while we will not get a good frequency response. Hence, usually a combination of the other resonators is used alongside the coupled lines. Accordingly, we propose the general structure shown in Fig. 1 to design the BPFs. As depicted in Fig. 1, it consists of coupled lines connected to a simple line loaded by a shunt internal resonator. To save the size, we placed the simple transmission line in such a way that it forms a U-shaped structure next to the coupled lines. The stub is loaded inside the U-shape structure to save the overall size again.

The impedance of the coupled lines and internal shunt stub are assumed to be Z_C and Z_S, respectively. As presented in Fig. 1, the transmission line is divided into two parts with the impedances Z_1 and Z_2. The input impedance that displayed from the input port is:

$$Z_{in} = \frac{Z_S Z_1}{Z_S + Z_1} + Z_C + Z_2 = \frac{Z_S Z_1 + Z_S Z_C + Z_S Z_2 + Z_1 Z_2 + Z_C Z_1}{Z_S + Z_1} \quad (1)$$

One way to create a resonance is to have $Z_S = -Z_1$ According to the proposed resonator structure, Z_1 is an impedance of an inductor. Therefore, the shunt stub must be capacitive. The fill square or rectangular cells are good choices for the internal stub. A larger internal stub shifts the resonance frequency to the lower frequencies. Another way to get the resonance frequency is:

$$Z_S(Z_1 + Z_C + Z_2) + Z_1(Z_2 + Z_C) = 0 \quad (2)$$

A method to solve Eq. (2) is by setting reasonable custom values for some parameters to find the other values easily. To calculate Z_1, we can use the following equations (Hong and Lancaster, 2001):

$$Z_1 = jZ_{C1} \tan(\beta l_1) \quad (3.a)$$

where:

$$Z_{C1} = \frac{120\pi}{\sqrt{\varepsilon_{re}}} \{\frac{w}{h} + 1.393 + 0.677 \ln(\frac{w}{h} + 1.444)\}^{-1} \quad (3.b)$$

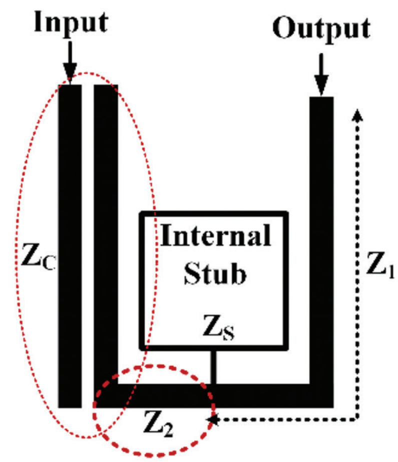

Fig. 1. Proposed resonator consisting of coupled lines connected to a simple line loaded by a shunt internal resonator.

$$\beta = \frac{\pi f_O(GHz)\sqrt{\varepsilon_{re}}}{150} \quad (3.c)$$

In Eq. (3), Z_{C1} and β are the characteristic impedance and propagation constant. If we assume that the length of the transmission line with the impedance Z_1 is l_1 = 20 mm with a width of W = 0.6 mm on a substrate with the effective dielectric constant of ε_{re} = 1.75 (ε_r = 2.22), Zc_1 become near 105.97Ω. On the other hand, at a target operational frequency of f_o = 2 GHz, β become near 17.63π. Finally, Z_1 = 211.94j Ω which is the equivalent of a 16.86 nH inductance. If the internal shunt stub is a large square fill cell with 10 mm × 10 mm dimension, the characteristic impedance of internal stub will be Z_{CS} = 17.9 Ω while β = 17.63π. In this case, Z_S must be calculated from:

$$Z_S = \frac{Z_{CS}}{j \tan(0.01\beta)} \quad (3.d)$$

So Z_S = −j28.9 Ω, which is equivalent of a capacitor. If we increase the size of internal stub to 20 mm × 20 mm, then Z_S = −14jΩ. Therefore, by increasing the dimension of the shunt stub it will be equal to a large capacitor which can shift the resonance frequency to the left. We can set Z_2 = 0.5 and Z_1 = 105.97jΩ to find the impedance of coupled lines easily. This was a method to solve Eq. (2). We can optimize the dimensions to obtain more compact size at our desired resonance frequency. Using this analyzed resonator, two BPFs can be designed as it is explained in the next section.

III. Design of BPFs

Based on the proposed resonator, two BPFs are designed for wireless applications. The first filter (BPF1) is shown in Fig. 2 which operates at the higher frequency. This filter is composed of coupled lines, simple transmission line and an internal shut stub.

The basic structure of this filter is the same as the analyzed resonator in the previous section. The internal stub is a high impedance section while two step-impedance feed structures are utilized to decrease the losses. The approximated

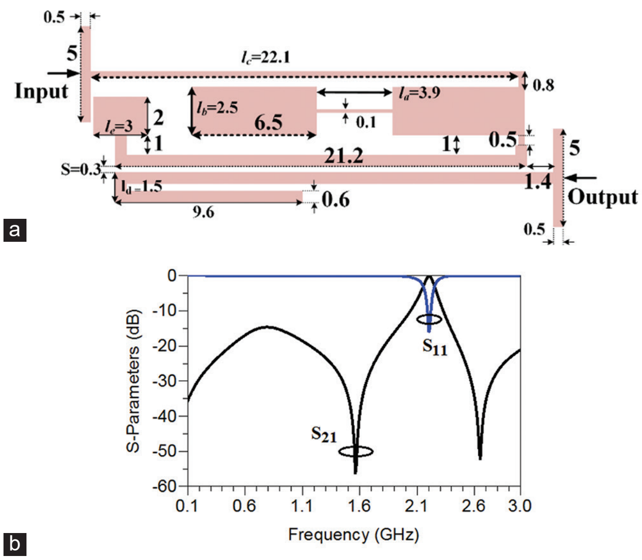

Fig. 2. (a) Layout of BPF1 (all dimensions are in mm), (b) Frequency response of BPF1.

dimensions are obtained according to the method explained in the Resonator Structure section. Then, we optimized the dimensions to get a better frequency response. Tapped line feeds are used to control the insertion loss and return loss, where the loss control is much easier to adjust.

It is simulated on a RT/Duroid 5880 substrate with 2.22 dielectric constant, h = 0.7874 mm and 0.0009 loss tangent. It is simulated by ADS software.

The resonance frequency of BPF1 is located at 2.2 GHz, with 0.23 dB insertion loss while the return loss is 16.1 dB. This filter creates two TZs at 1.56 GHz and 2.65 GHz which improve the selectivity. The harmonic level is lower than 14.6 dB above and after the passband up to 3 GHz. The dimensions of BPF1 are optimized as presented in Fig. 3a-f. Fig. 3a shows S_{21} and S_{11} as a function of the physical length l_a. By increasing this length, the operational frequency shifts to the lower frequency. As depicted in Fig. 3a, increasing the length l_a will also lead to improve selectivity. However, better return loss will be obtained by decreasing l_a. Fig. 3b

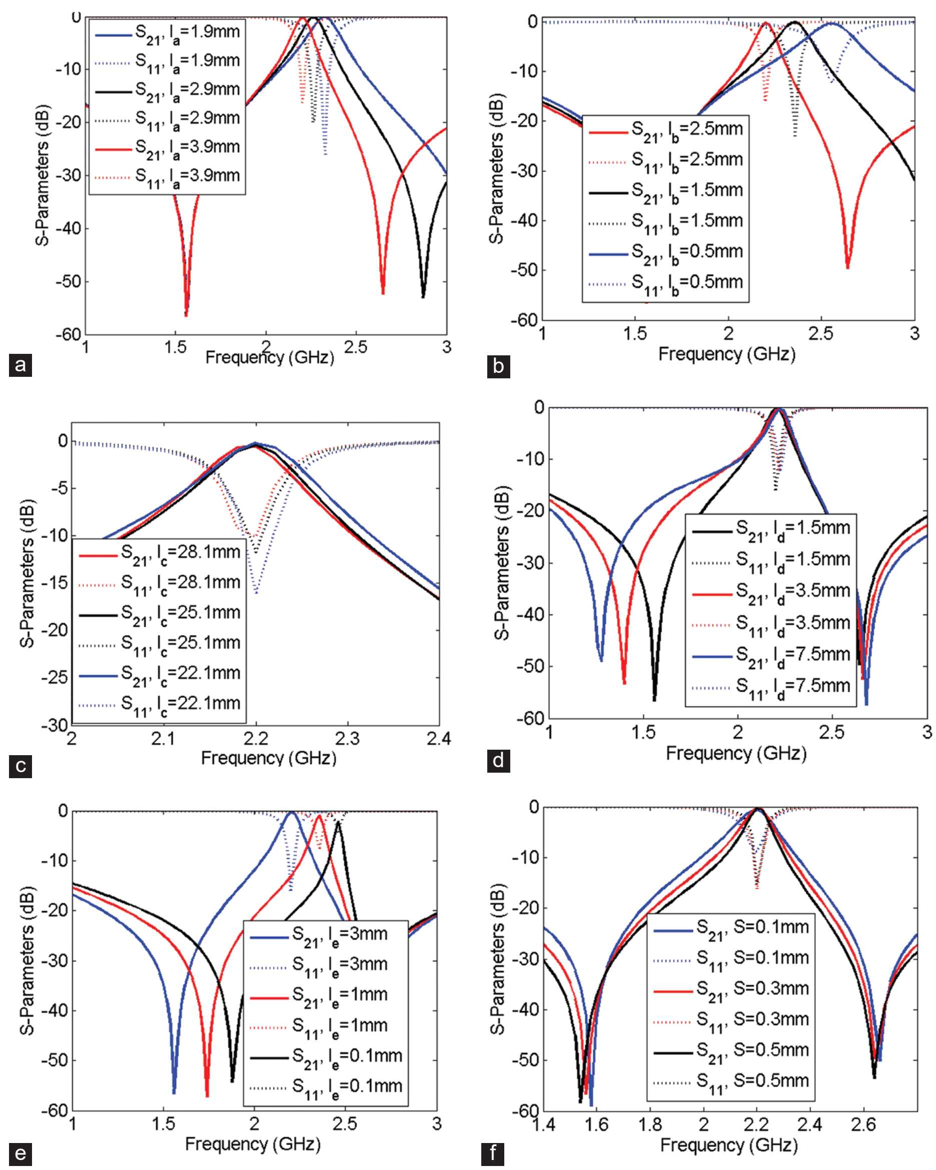

Fig. 3. Frequency response as a function of (a) l_a, (b) l_b, (c) l_c, (d) l_d, (e) l_e and (f) S.

http://dx.doi.org/10.14500/aro.10999

illustrates the frequency response of BPF1 as a function of length l_b. Similar to the effect of l_a, increasing the size of l_b shifts the resonant frequency to the left. On the other hand, decreasing l_b will increase the bandwidth. Therefore, it is wise to choose an intermediate value of l_b. As shown in Fig. 3c, we can decrease the physical length l_b to improve the return loss. However, if we reduce it too much, the frequency response will be broken or at least the resonance frequency will shift to the right. As presented in Fig. 3d, to improve the sharpness of the frequency response, the length l_d can be reduced. Decreasing the physical length l_e will corrupt the frequency response. This is presented in Fig. 3e. As shown in Fig. 3e, by increasing l_e the losses are decreased significantly. The distance between the coupled lines has a significant effect on the return loss. This is shown in Fig. 3f, where by reducing S, the return loss will be increased.

From the above optimization method, it can be concluded that increasing the dimensions will lead to a resonance frequency shifted to the left. However, we must be careful not to destroy the other features by increasing the dimensions. Using the above method, another BPF named as BPF2 is designed to operate at lower frequencies. The layout configuration of BPF2 and its corresponding frequency response are depicted in Fig. 4a and b. As shown in Fig. 4a, the coupled lines and shunt stub are used similar to our proposed resonator. Here, the shunt stub is a rectangular cell.

Similar to the proposed resonator, BPF2 is composed of a pair of coupled lines and a shunt stub. Another rectangular stub is connected to the upper line to control the bandwidth. The main shunt stub with physical length l_i is important to form the bandwidth. Similar to the BPF1, tapped line feeds are used to control the insertion and return losses easily. The approximated dimensions can calculate according to the explained method in the resonator design.

To optimize the frequency response, the other stubs are added. Fig. 4b depicts that BPF2 operates at 870 MHz which is suitable for GSM applications.

The passband is from 790 MHz to 950 MHz with 0.57 dB insertion loss. The effect of changing BPFs parameters is presented in Fig. 5a-d. Fig. 5a and b show that two factors can eliminate passband. One of them is decreasing the physical length l_f and the other one is decreasing the length l_g. As depicted in Fig. 5a, choosing a neither low nor high value of l_f is suitable. The length l_g has a similar effect so that we must choose a middle value of it. Increasing the physical lengths l_h and l_i can improve the frequency selectivity. The effect of these lengths on the frequency response is presented in Fig. 5c and d. Moreover, decreasing these lengths increases the losses. Therefore, we can enlarge l_h and l_i insofar as the overall size remains compact. By connecting both BPF1 and BPF2, a microstrip diplexer is designed, as shown in the next section.

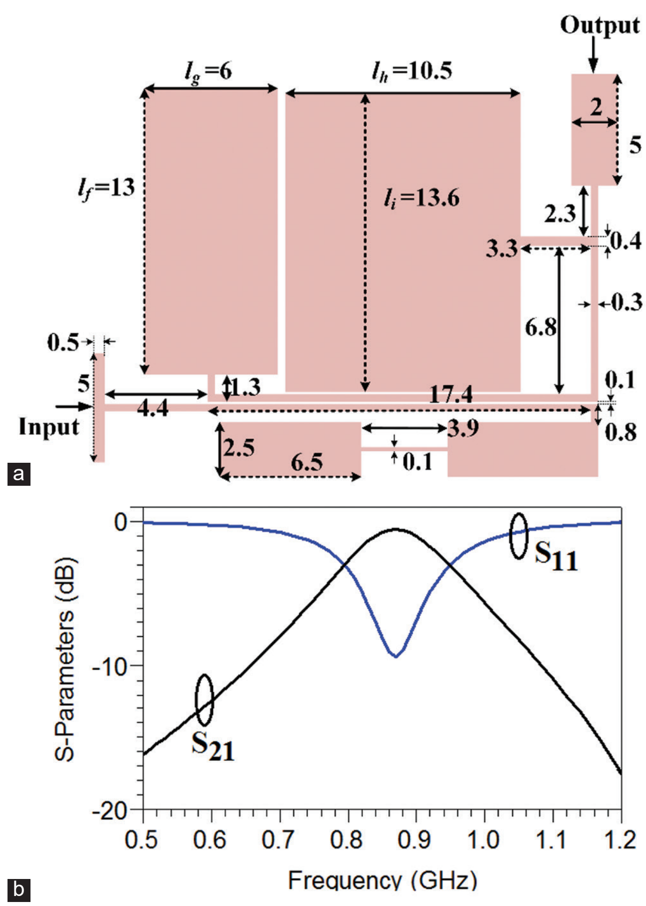

Fig. 4. (a) Layout configuration of BPF2 where all dimensions are in mm, (b) frequency response of BPF2.

IV. Diplexer Structure and Its Simulation Results

A microstrip diplexer usually is composed of two BPFs. In some cases, a matching network is used to obtain a good performance. However, we connected our both filters without any extra matching network that leads to save the size. Our proposed diplexer is presented in Fig. 6.

This diplexer is made by direct connection of BPF1 and BPF2. As shown in Fig. 6, the BPF1 and BPF2 are connected to Port3 and Port2, respectively. According

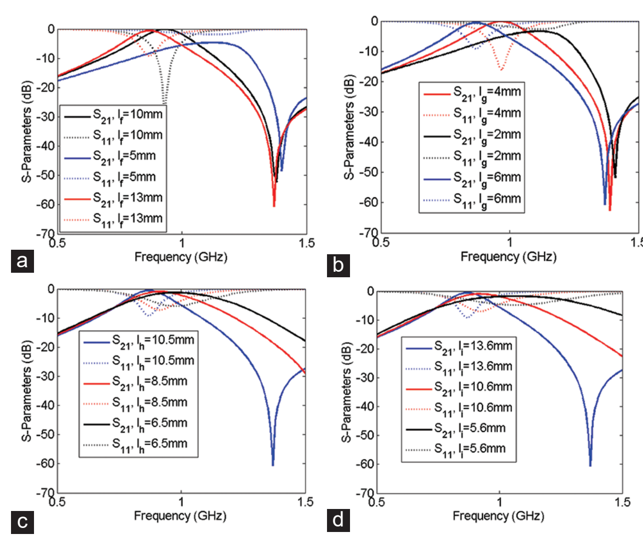

Fig. 5. Frequency response of BPF2 as functions of (a) l_f, (b) l_g, (c) l_h, (d) l_i.

to the optimization method in the previous section, the dimensions are selected so that we have the best frequency response. The high impedance part is repeated in both filters. However, it is seen once in the proposed diplexer structure which leads to save size significantly. The overall size of our designed diplexer is 22.9 mm × 25 mm ($0.09\lambda_g \times 0.098\lambda_g$) which is very compact, where λ_g is the guided wavelength on the substrate calculated at the lower resonance frequency. The overall size according to the second resonance frequency is $0.22\lambda_{g\text{-}s} \times 0.24\,\lambda_{g\text{-}s}$, where $\lambda_{g\text{-}s}$ is the guided wavelength on the substrate calculated at the upper resonance frequency.

The frequency response of the proposed diplexer is depicted in Fig. 7a and b. Both filters and the proposed diplexer are simulated on a RT/Duroid 5880 substrate with $\varepsilon_r = 2.22$, h = 0.7874 mm and 0.0009 loss tangent.

The simulation results are extracted by Agilent Advanced Design System (ADS) software using the EM simulator. As illustrated in Fig. 7a, the first passband is from 735 MHz to 1005 MHz. The fractional bandwidth (FBW) at this channel is 31%. Therefore, this channel is wide which is an advantage. The resonance frequency of this channel is f_{o1} = 895 MHz, which is suitable for GSM applications. The losses in this channel are very low. The simulated insertion and return losses are 0.075 dB and 40.3 dB respectively. Fig. 7a shows that there is an 80.2 dB TZ at 1.494 GHz which improves the sharpness of the first channel. Similar to the lower channel, our upper channel has low losses with 0.14 dB insertion loss and 31.7 dB return loss. The upper operational frequency is f_{o1} = 2.2 GHz. This passband is from 2.14 GHz to 2.26 GHz with 5.45% FBW. S_{31} has two TZs of 60.6 dB and 55.954 dB at 1.564 GHz and 2.683 GHz respectively. As shown in Fig. 7, the harmonics are suppressed up to 3 GHz where it has the maximum harmonic level 14.6 dB. Fig. 7b depicts the isolation between channels which is better than 20.71 dB from DC to 3 GHz.

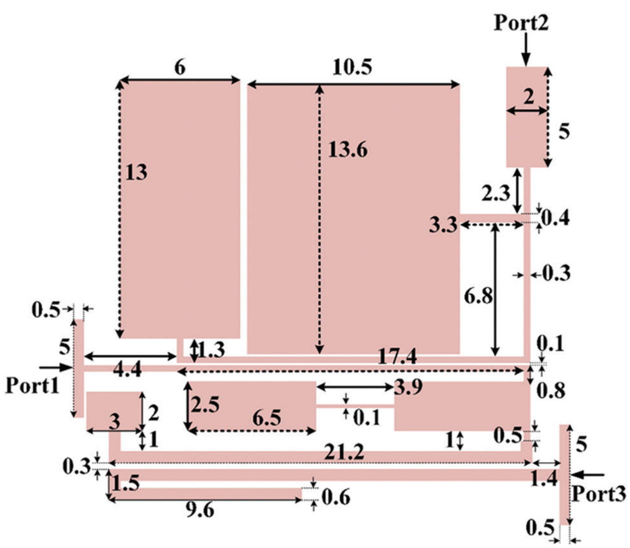

Fig. 6. Layout of the proposed diplexer where all dimensions are in mm.

V. Comparison and Discussion

To show the advantages of this work, we compared it with the previous diplexers. The comparison results are listed in Table I, where IL1, IL2, RL1, and RL2 are insertion loss at the first channel, insertion loss at the second channel, return loss at the first channel and return loss at the second channel, respectively. As shown in Table I, the lowest insertion loss at the first channel and the lowest common port return loss at both channels are the achievements of this work. Another significant advantage of our diplexer is to have the most compact size in comparison with the previous diplexers. As illustrated in Table I, we could get an acceptable harmonic attenuation. Only the introduced diplexer in (Yahya, Rezaei and Nouri, 2020) could attenuate better than us. However, it has a very large size of 0.037 λg^2 with high common port return loss at its both channels.

In the comparison table, the data of these works: (Hussein, Mezaal and Alameri, 2021), (Yahya, Rezaei and Nouri, 2020), (Tahmasbi, Razaghian and Roshani, 2021), (Rezaei, et al., 2019), (Shirkhar and Roshani, 2021), (Rezaei, et al., 2019), (Fernandez-Prieto, et al., 2018), and (Noori and Rezaei, 2017) are based on simulation results and the others are based on the measured results. As shown in Table I, our diplexer has low loss, compact size, good harmonic attenuation, and reasonable isolation.

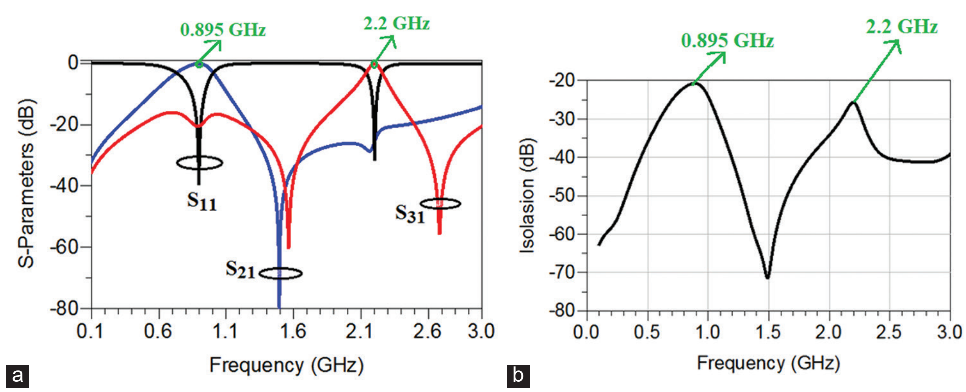

Fig. 7. Frequency response of the proposed diplexer (a) transfer parameters and common port return loss, (b) isolation between channels.

Table I
Comparison between this Work and the Previously Reported Diplexers

References	Common port insertion losses: IL_1, IL_2 (dB)	Common port return losses: RL_1, RL_2 (dB)	f_{o1}, f_{o2} (GHz)	Size (λg^2)	Last suppressed harmonic	Isolation (dB)
Our Diplexer	0.075, 0.14	40.3, 31.77	0.895, 2.2	0.008	3.3 f_{o1}	20.7
(Hussein, Mezaal and Alameri, 2021)	4.2, 3.3	32, 31	1.85, 2.5	0.096	1.6 f_{o1}	31
(Chen et al., 2021)	4.4, 4.6	Better than 15	1.41, 2.02	0.098	3 f_{o1}	29
(Yahya, Rezaei and Nouri, 2020)	0.12, 0.18	21, 17	3.5, 5	0.037	12 f_{o1}	20
(Lu, et al., 2020)	0.8, 1.1	---	0.755, 1.056	0.040	2.1 f_{o1}	24
(Su, et al., 2020)	2.62, 2.34	---	9.55, 10.61	3.56	2.1 f_{o1}	45
(Tahmasbi, Razaghian and Roshani, 2021)	0.05, 0.08	26.9, 23.5	1.5, 2.1	0.030	3.3 f_{o1}	19
(Rezaei, et al., 2019)	0.36, 0.44	23.7, 23.7	2.88, 3.29	0.028	1.2 f_{o1}	23
(Shirkhar and Roshani, 2021)	Better than 0.5	20, 25	1.7, 2.1	0.061	1.4 f_{o1}	40
(Zhanga, Zhu and Li, 2018)	1.06, 1.09	Better than 17	2.2, 2.63	0.207	1.8 f_{o1}	38
(Rezaei, et al., 2019)	0.10, 0.16	33, 22	1.6, 2.1	0.054	2.1 f_{o1}	22
(Dembele, et al., 2019)	1.8, 1.9	10, 10	8.3, 10	0.071	2.4 f_{o1}	26.6
(Yousif and Ezzulddin, 2020)	0.5, 2	16, 25	2.6, 6	0.22*	3 f_{o1}	23
(Fernandez-Prieto, et al., 2018)	1.15, 1.54	Near 30	2.49, 2.97	0.218	4 f_{o1}	30
(Guan, et al., 2019)	1.15, 1.5	Better than 17.7	0.99, 1.46	0.097	2.5 f_{o1}	40
(Guan, et al., 2014)	1.2, 1.5	Near 20	1.95, 2.14	0.136	1.2 f_{o1}	35
(Noori and Rezaei, 2017)	0.2, 0.4	15, 11	2.36, 4	0.089	3.3 f_{o1}	19.8

*Approximate

VI. Conclusion

A microstrip diplexer, composed of two BPFs, is introduced in this work. The resonance frequency of the filters and diplexer make them suitable for modern wireless communication networks. First, a resonator, and then, two BPFs were proposed and optimized. Finally, by connecting the BPFs without any extra matching circuit a high performance diplexer was introduced. Both passbands presented good features. The comparison results of the proposed new design approach with the previously reported designs showed that the lowest insertion loss at the lower channel and the lowest return losses at both channels are obtained while our diplexer has the most compact size. Meanwhile, the other parameters such as FBW at the first channel (31%) and harmonic attenuation were good. The isolation and FBW at the upper band were acceptable.

References

Chen, C.F., Zhou, K.W., Chen, R.Y., Tseng, H.Y., He, Y.H., Li, W.J. and Weng, J.H., 2021. Design of microstrip multifunction integrated diplexers with frequency division, frequency selection, and power division functions. *IEEE Access*, 9, pp.53232-53242.

Dembele, S.N., Bao, J., Zhang, T. and Bukuru, D., 2019. Compact microstrip diplexer based on dual closed loop stepped impedance resonator. *Progress in Electromagnetics Research C*, 89, pp.233-241.

Fernandez-Prieto, A., Lujambio, A., Martel, J., Medina, F., Martin, F. and Boix, R.R., 2018. Balanced-to-balanced microstrip diplexer based on magnetically coupled resonators. *IEEE Access*, 6, pp.18536-18547.

Guan, X., Liu, W., Ren, B., Liu, H. and Wen, P., 2019. A novel design method for high isolated microstrip diplexers without extra matching circuit. IEEE Access, 7, pp.119681-119688.

Guan, X., Member, F., Yang, H., Liu, H. and Zhu, L., 2014. Compact and high-isolation diplexer using dual-mode stub-loaded resonators. *IEEE Microwave and Wireless Components Letters*, 24(6), pp.385-387.

Hong, J.S. and Lancaster, M.J., 2001. *Microstrip Filters for Rf/Microwave Applications*. John Wiley and Sons, Hoboken.

Hussein, H.A., Mezaal, Y.S. and Alameri, B.M., 2021. Miniaturized microstrip diplexer based on fr4 substrate for wireless communications. *Elektronika Ir Elektrotechnika*, 27(5), pp.34-40.

Lu, Q.Y., Zhang, Y.J., Cai, J., Qin, W. and Chen, J.X., 2020. Microstrip tunable diplexer with separately-designable channels. *IEEE Transactions on Circuits and Systems II: Express Briefs*, 67(12), pp.2983-2987.

Majdi, K.A. and Mezaal, Y.S., 2022. Microstrip diplexer for recent wireless communities. *Periodicals of Engineering and Natural Sciences*, 10(1), pp.387-396.

Noori, L., Rezaei, A., 2017. Design of a microstrip dual-frequency diplexer using microstrip cells analysis and coupled lines components. International Journal of Microwave and Wireless Technologies, 9(7), pp.1467-1471.

Rezaei, A., Noori, L. and Mohammadi, H., 2019. Design of a miniaturized microstrip diplexer using coupled lines and spiral structures for wireless and WiMAX applications. Analog Integrated Circuits and Signal Processing, 98, pp.409-415.

Rezaei, A., Yahya, S.I., Noori, L. and Jamaluddin, M.H., 2019. Design of a novel wideband microstrip diplexer using artificial neural network. *Analog Integrated Circuits and Signal Processing*, 101(1), pp.57-66.

Shirkhar, M.M. and Roshani, S., 2021. Design and implementation of a Bandpass-bandpass diplexer using coupled structures. *Wireless Personal Communications*, 122(3), pp.2463-2477.

Su, Z.L., Xu, B.W., Zheng, S.Y., Liu, H.W. and Long, Y.L., 2020. High-isolation and Wide-stopband SIW diplexer using mixed electric and magnetic coupling. IEEE Transactions on Circuits and Systems II: Express Briefs, 67(1), pp.32-36.

Tahmasbi, M., Razaghian, F. and Roshani, S., 2021. Design of bandpass-bandpass diplexers using rectangular-, T-, and Lshaped resonators for hybrid power amplifier and 5G applications. *Analog Integrated Circuits and Signal Processing*, 109(3), pp.585-597.

Yahya, S.I., Rezaei, A. and Nouri, L., 2020. Compact wide stopband microstrip diplexer with flat channels for WiMAX and wireless applications. IET Circuits, Devices *and* Systems, 14(6), pp.846-852.

Yousif, A.B. and Ezzulddin, A.S., 2020. A Dual-band coupled line based microstrip diplexer for wireless applications. *Journal of Global Scientific Research*, 10, pp.845-853.

Zhanga, C., Zhu, L. and Li, Y., 2018. Compact microstrip balanced-to-balanced diplexer using stub-loaded dual-mode resonators. *IEICE Electronics Express*, 15(5), pp.1-6.